Ultrafast Dephasing of Coherent Intersubband Polarizations in a Quasi-Two-Dimensional Electron Plasma

Robert A. Kaindl, Stephan Lutgen, Michael Woerner, and Thomas Elsaesser

Max-Born-Institut für Nichtlineare Optik und Kurzzeitspektroskopie, D-12489 Berlin, Germany

Bernd Nottelmann, Vollrath Martin Axt, and Tilmann Kuhn

Institut für Theoretische Physik II, Westfälische Wilhelms-Universität, D-48149 Münster, Germany

Andreas Hase and Harald Künzel

Heinrich-Hertz-Institut für Nachrichtentechnik Berlin GmbH, D-10587 Berlin, Germany

We present the first study of coherent intersubband polarizations in a pure electron plasma by femtosecond four-wave mixing in the midinfrared. Resonantly excited polarizations between consecutive conduction subbands of narrow GaInAs/AlInAs quantum wells decay within about 500 fs, much faster than intersubband relaxation of electrons. The relation between the decay rate of the signals and the dephasing rate is analyzed by solving the time-dependent Hartree-Fock equations for the single-particle density matrix. Electron-electron scattering is identified as the main dephasing mechanism. [S0031-9007(98)05833-5]

PACS numbers: 73.20.Dx, 42.65.Re, 78.47.+p

The optical properties and the dynamics of elementary excitations of a low-dimensional electron gas are distinctly different from spatially homogeneous bulk materials. In semiconductor quantum wells (QW's), the quantum confinement of carriers to a quasi-two-dimensional (2D) geometry leads to a sequence of discrete valence and conduction subbands and a novel elementary excitation, the optical intersubband (IS) transition between consecutive bands which occurs in the infrared spectral range below the fundamental band gap. IS excitations play an important role for the ultrafast nonequilibrium dynamics of carriers in QW's [1] and for device applications like the quantum cascade laser [2]. Until now, processes mainly of carrier redistribution after IS excitation, i.e., *population relaxation,* have been studied. For energy spacings of the $n = 1$ and $n = 2$ conduction subbands higher than the energy of optical phonons, the lifetime of $n = 2$ electrons has a value of about 1 ps, determined by IS scattering with longitudinal optical (LO) phonons [3,4]. On a similar time scale, a quasiequilibrium electron distribution in the lower subband is formed [4].

Resonant IS excitation by coherent infrared radiation creates a coherent optical IS polarization which decays irreversibly by phase-breaking scattering processes. In contrast to population relaxation, this *phase relaxation* has been much less explored. The time scale and the mechanisms of the loss of IS phase coherence are not well understood. Moreover, the time-dependent many-body effects during phase relaxation and the homogeneous broadening of IS absorption profiles are barely characterized. In a recent experiment carried out at room temperature, a coherent IS polarization was created by femtosecond interband excitation of asymmetric QW's. The decay of

the macroscopic polarization was monitored via the electric field transients emitted by the sample and occurred with time constants of 110 to 180 fs [5]. In this experiment, both the destructive interference between different components of the inhomogeneously broadened ensemble and the irreversible phase relaxation due to scattering mechanisms are responsible for the decay and cannot be separated. Moreover, electron-electron, electron-hole, and carrier-phonon scattering are expected to contribute to phase relaxation after broadband interband excitation. Because of this complex situation, an analysis of the relevant scattering processes has not been possible. Here, experiments with single component plasmas, e.g., of electrons, should provide more specific information.

In this Letter, we report a femtosecond study of coherent intersubband polarizations in a pure electron plasma. The dynamics of IS phase relaxation in n-type modulation-doped $Ga_{0.47}In_{0.53}As/Al_{0.48}In_{0.52}As$ quantum wells is investigated by time-resolved four-wave mixing (FWM) in the midinfrared. Our measurements for a broad range of electron densities demonstrate for the first time that electron-electron scattering represents the dominant mechanism of phase relaxation occurring on a time scale of several hundreds of femtoseconds. FWM signals are modeled theoretically by solving the time-dependent Hartree-Fock equations for the one-particle density matrix, giving insight into the many-body effects and the role of inhomogeneous broadening for the decay of the signal.

In the experiments, we study n-type modulation-doped $Ga_{0.47}In_{0.53}As/Al_{0.48}In_{0.52}As$ multiple quantum wells grown by molecular beam epitaxy on an InP substrate. They consist of $50\,Ga_{0.47}In_{0.53}As$ QW's of 6 nm width

separated by 14 nm wide $Al_{0.48}In_{0.52}As$ barriers which are Si delta doped in the centers. Three samples with doping densities of $n_S = 1.5 \times 10^{11}$ cm^{-2}, 5×10^{11} cm^{-2}, and 1.5×10^{12} cm^{-2} are investigated. The $n = 1$ to $n = 2$ IS absorption spectrum of the first sample is centered at 257 meV with a linewidth (FWHM) of 14 meV (inset of Fig. 1). For the time-resolved experiments, nearly transform-limited midinfrared pulses resonant to the IS transition are generated by parametric frequency mixing (pulse duration 130 fs, bandwidth 15 meV) [6]. In a standard FWM geometry, two pulses with wave vectors $\mathbf{k}_1$ and $\mathbf{k}_2$ create a transient grating in the sample from which third order nonlinear signals are generated by self-diffraction into the directions $2\mathbf{k}_2 - \mathbf{k}_1$ and $2\mathbf{k}_1 - \mathbf{k}_2$. The two signals, which are symmetric in time with respect to zero pulse delay, were detected by InSb detectors, either spectrally integrated or resolved (resolution 2 meV). A prism geometry of the sample was used to achieve maximum overlap of the in-plane electric field vector of the pulses with the IS dipole moment oriented perpendicular to the QW's.

In Fig. 1, we present FWM signals for different electron densities. The spectrally integrated intensity diffracted into the direction $2\mathbf{k}_2 - \mathbf{k}_1$ is plotted on a logarithmic scale as a function of delay time between the two pulses generating the transient grating. The dashed line gives the cross correlation of the two pulses measured in a thin AgGaS$_2$ crystal. At low density [Fig. 1(a)], the signal rises within the time resolution of the experiment, reaches a maximum after 100 fs, and decays within 700 fs. A numerical monoexponential fit gives a decay time of 80 ± 15 fs. With increasing density [Figs. 1(b) and 1(c)], the maximum of the signal shifts towards delay zero and the decay becomes faster. For electron densities of $n_S = 5 \times 10^{11}$ and $n_S = 1.5 \times 10^{12}$ cm^{-2}, the respective decay times are 65 fs and ≤ 50 fs. In such measurements, about 20% of the electrons in the respective sample were excited to the $n = 2$ subband, as estimated from the pulse intensity (peak intensity $I_0 = 5$ MW/cm^2) and the IS absorbance. For pulse intensities between $I_0/2$ to $2I_0$, the temporal shape of the FWM curves remains unchanged and the signal strength follows $(I_0)^3$, as expected for a third order process. In addition to the time evolution, we studied the spectral distribution of the diffracted intensity. The spectrum in the inset of Fig. 1(a) (symbols) shows the resonant enhancement of the signal at the IS transition. The change of the FWM signals with the lattice temperature T_L was studied for the sample with $n_S = 1.5 \times 10^{11}$ cm^{-2} (Fig. 2). The decay rates increase
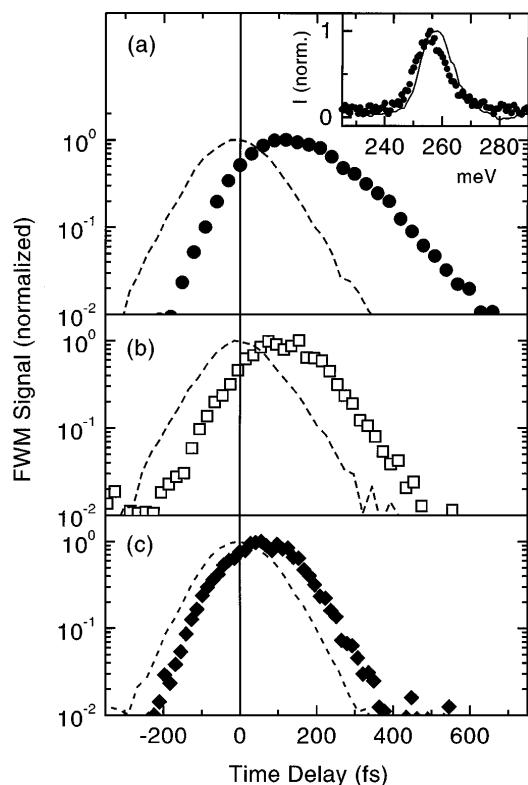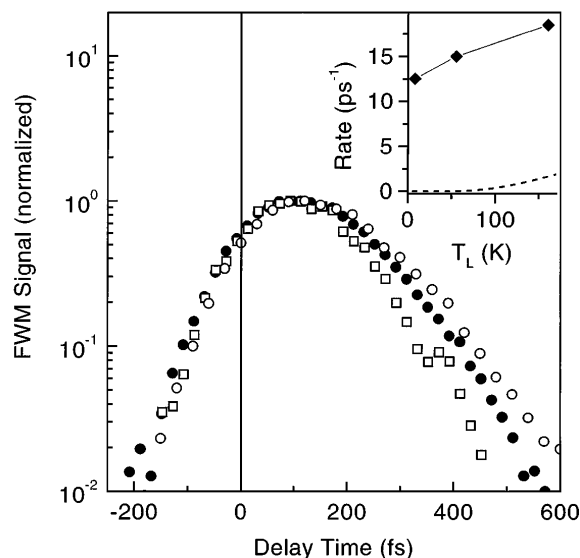

FIG. 1. Four-wave mixing signals recorded with femtosecond excitation resonant to the intersubband transition in the midinfrared. The intensity diffracted from the transient grating in the sample is plotted as a function of delay time between the two pulses generating the grating (lattice temperature $T_L = 8$ K). (a) Data for an electron concentration of $n_S = 1.5 \times 10^{11}$ cm^{-2} (symbols). The dashed line gives the cross correlation of the two femtosecond pulses. Inset: Intersubband absorption spectrum (solid line) and spectrum of the FWM signal at delay zero (symbols). (b),(c) Data for $n_S = 5 \times 10^{11}$ cm^{-2} and $n_S = 1.5 \times 10^{12}$ cm^{-2}.

FIG. 2. Spectrally integrated four-wave mixing signals for $n_S = 1.5 \times 10^{11}$ cm^{-2} and lattice temperatures of $T_L = 8$ K (open circles), 55 K (solid circles), and 160 K (open boxes). Inset: Decay rates of the FWM signals for different T_L (symbols). Dashed line: LO phonon absorption rate as estimated from the temperature-dependent phonon occupation number.

by a factor of about 1.5 when raising T_L from 8 to 160 K (Fig. 2, inset).

The FWM signals in Figs. 1 and 2 exhibit essentially monoexponential decays with time constants between ≤ 50 and 80 fs. Such dynamics are much faster than IS relaxation of photoexcited electrons from the $n = 2$ back to the $n = 1$ subband. Time-resolved infrared measurements of nonlinear IS absorption in the same three samples gave IS scattering times of 1.3 ps determined by LO phonon emission [7,8]. Thus, IS population relaxation plays a minor role for dephasing. Instead, electron-electron, intraband electron-LO phonon scattering and—to a minor extent—electron-impurity scattering are potential mechanisms which determine the phase relaxation time T_2 and lead to a homogeneous broadening of the IS transition. In addition, QW thickness and alloy fluctuations and the different dispersion of the two subbands in k space result in inhomogeneous broadening [7,9]. The excitation bandwidth in our experiments is close to the spectral width of IS absorption, i.e., this distribution of IS transition frequencies is excited phase coherently and contributes to the overall polarization.

In the simplest theoretical description based on independent two-level systems, the FWM signal from a homogeneously and inhomogeneously broadened ensemble decays with time constants of $T_2/2$ and $T_2/4$, respectively. For IS excitations, however, the coupling of the transition dipoles by many-body effects requires a more sophisticated theoretical treatment. To get insight into such phenomena, we performed calculations based on the time dependent Hartree-Fock equations (TDHF) which account for many-body effects on a mean-field level and allow for a simultaneous study of inhomogeneous broadening [9–12]. To analyze the different factors influencing the signal, we numerically studied the following four cases: (i) Two-band model with equal effective electron masses $m_1 = m_2 = 0.05m_0$ in the two subbands (m_0: free electron mass). The system was assumed to be exclusively homogeneously broadened with a constant, k-independent dephasing time T_2, and the Coulomb interaction was switched off. The other cases correspond to adding successively (ii) the Coulomb interaction (many-body effects), (iii) the effect of different masses in the subbands ($m_1 = 0.05m_0, m_2 = 0.065m_0$) [7], and (iv) the influence of (Gaussian) inhomogeneous broadening $\Delta\omega_G$ due to QW thickness and alloy fluctuations ($\Delta\omega_G = 12$ meV). For the different doping densities, first the correct ground state was determined, and then the FWM signals in the directions $2\mathbf{k}_2 - \mathbf{k}_1$ and $2\mathbf{k}_1 - \mathbf{k}_2$ were calculated as a function of delay time.

Figure 3 shows the results for the lowest and highest doping density with respective T_2 values of 310 and 100 fs. In the noninteracting, homogeneously broadened case a decay rate of $T_2/2$ is found. With increasing complexity, the decay becomes faster and a value of $T_2/4$ is approached. The importance of the different contributions varies strongly from the low to the high den-
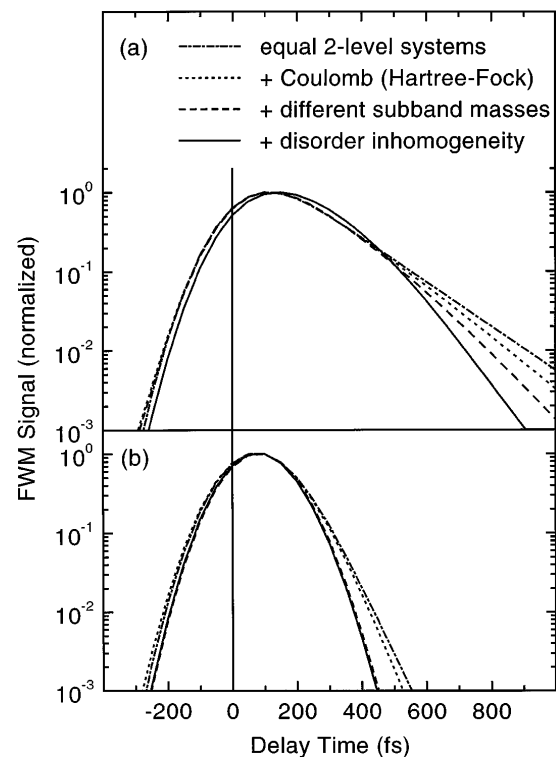

FIG. 3. Theoretical results for the spectrally integrated four-wave mixing signals obtained from the TDHF equations for different model cases (lattice temperature $T_L = 8$ K). (a) Electron density $n_S = 1.5 \times 10^{11}$ cm^{-2}, dephasing time $T_2 = 310$ fs. (b) Electron density $n_S = 1.5 \times 10^{12}$ cm^{-2}, $T_2 = 100$ fs.

sity. If we define the decay time as T_2/α, we find at the low density the values (i) $\alpha = 2.0$, (ii) $\alpha = 2.3$, (iii) $\alpha = 2.9$, and (iv) $\alpha = 3.9$, while at the high density we find (i) $\alpha = 2.0$, (ii) $\alpha = 2.4$, (iii) $\alpha = 4.0$, and (iv) $\alpha = 4.0$. Coulomb interaction leads to a nonparabolic dispersion in the Hartree-Fock ground state below the Fermi energy [11]. While in the low density case Coulomb interaction and different masses enhance the decay rate by about 50%, at high density they already lead to values close to $4/T_2$. Here, additional inhomogeneous broadening does not further enhance the decay. Taking into account such theoretical results, the width of the IS absorption lines in our samples, and the measured decay rates, we conclude that the FWM signals decay with $4/T_2$. This gives dephasing times $T_2 \simeq 320$ and ≤ 200 fs for the lowest and the highest electron density. The corresponding homogeneous linewidth for low carrier density has a value of 4 meV, representing about 30% of the total linewidth.

We now address the scattering processes relevant for IS dephasing. In our modulation-doped samples, the electron gas in the QW's is spatially separated from the ionized donors in the barriers, resulting in characteristic scattering times of 1–2 ps [13], much longer than the

dephasing times. For $T_L = 8$ K (cf. Fig. 1), the thermal LO phonon population and, thus, LO phonon absorption by electrons are negligible. For an electron density of $n_S = 1.5 \times 10^{11}$ cm^{-2}, the Fermi energy of $E_F = 7$ meV is much smaller than the LO phonon energy of $E_{LO} \simeq 30$ meV. Resonant IS excitation promotes electrons to states close to the bottom of the $n = 2$ subband, well below E_{LO}. Thus, LO phonon emission is suppressed in both subbands, and the contribution of intraband LO phonon scattering to the fast dephasing is negligible [14].

Under such conditions, electron-electron scattering represents the main dephasing mechanism. The increase of the dephasing rate with carrier density (Fig. 1) is due mainly to the rise of electron-electron scattering rates. Intraband scattering in the $n = 1$ and $n = 2$ subbands and scattering events where an electron in one subband interacts with an electron in the other subband and each carrier is scattered to a final state in its own subband represent the main contributions to the overall scattering rate. Because of the different symmetry of the $n = 1$ and $n = 2$ electron wave functions, the rates of such processes are much higher than for scattering involving IS transfer of carriers [15]. Electron-electron scattering rates have been calculated for different electron distributions and different types of screening of the Coulomb interaction [16–18]. For 2D electron densities around 10^{11} cm^{-2} and carrier energies of up to 10 meV, electron-electron scattering leads to dephasing times of several hundred femtoseconds for valence to conduction band transitions [17], a time scale similar to that of IS dephasing reported here. It should be noted, however, that a theoretical analysis of IS dephasing by electron-electron scattering has not been performed until now.

A comment should be made on the temperature dependence of the dephasing rates, displaying a moderate increase with lattice temperature T_L (Fig. 2). This is due mainly to the thermal broadening of the electron distribution, reducing Pauli blocking of electron states. This makes a bigger part of phase space available for electron-electron scattering and enhances the dephasing rates. The increase of LO phonon population with T_L and the concomitant rise of the LO phonon absorption rate plays a minor role. This rate plotted in the inset of Fig. 2 (dashed line) is substantially lower than the observed dephasing rates.

In conclusion, the ultrafast dephasing of IS excitations in a pure electron plasma was studied for the first time using femtosecond four-wave mixing in the midinfrared. The decay of coherent IS polarizations in GaInAs/AlInAs

quantum wells occurs on a time scale of several hundreds of femtoseconds with dephasing rates increasing with carrier concentration and with temperature. Theoretical calculations based on the TDHF equations allow one to relate the decay rate of the signal with the IS dephasing rate and, thus, to determine the homogeneous contribution to the linewidth of IS absorption spectra. Our results clearly demonstrate that electron-electron scattering represents the dominant dephasing mechanism.

[1] For a review, *Intersubband Transitions in Quantum Wells*, edited by E. Rosencher *et al.* (Plenum Press, New York, 1992).

[2] J. Faist, F. Capasso, C. Sirtori, D. L. Sivco, A. L. Hutchinson, M. S. Hybertsen, and A. Y. Cho, Phys. Rev. Lett. **76**, 411 (1996).

[3] M. C. Tatham, J. F. Ryan, and C. T. Foxon, Phys. Rev. Lett. **63**, 1637 (1989).

[4] S. Lutgen, R. A. Kaindl, M. Woerner, T. Elsaesser, M. Gulia, D. Meglio, P. Lugli, A. Hase, and H. Künzel, Phys. Rev. Lett. **77**, 3657 (1996).

[5] A. Bonvalet, J. Nagle, V. Berger, A. Migus, J. L. Martin, and M. Joffre, Phys. Rev. Lett. **76**, 4392 (1996).

[6] F. Seifert, V. Petrov, and M. Woerner, Opt. Lett. **19**, 2009 (1994).

[7] S. Lutgen, R. A. Kaindl, M. Woerner, T. Elsaesser, A. Hase, and H. Künzel, Phys. Rev. B **54**, R17 343 (1996).

[8] S. Lutgen *et al.* (unpublished).

[9] M. Zaluzny, Phys. Rev. B **43**, 4511 (1991).

[10] In the case of interband dynamics in an intrinsic semiconductor, TDHF coincides with the semiconductor Bloch equations.

[11] M. S.-C. Luo, S. L. Chuang, S. Schmitt-Rink, and A. Pinczuk, Phys. Rev. B **48**, 11 086 (1993). In this reference only the $T = 0$ ground state has been calculated.

[12] F. Szmulowicz, M. O. Manasreh, C. E. Stutz, and T. Vaughan, Phys. Rev. B **50**, 11 618 (1994).

[13] M. A. Tischler, Appl. Phys. Lett. **58**, 1614 (1991).

[14] For a density $n_S = 5 \times 10^{11}$ cm^{-2} ($E_F = 18$ meV), LO phonon emission is still inhibited. For $n_S = 1.5 \times 10^{12}$ cm^{-2} ($E_F = 50$ meV), IS excitation creates a carrier distribution in which about 30% of the electrons can emit LO phonons.

[15] S. M. Goodnick and P. Lugli, Phys. Rev. B **37**, 2578 (1988).

[16] R. Binder, D. Scott, A. E. Paul, M. Lindberg, K. Henneberger, and S. W. Koch, Phys. Rev. B **45**, 1107 (1992).

[17] P. Hawrylak, J. F. Young, and P. Brockmann, Semicond. Sci. Technol. **9**, 432 (1994).

[18] K. ElSayed, L. Banyai, and H. Haug, Phys. Rev. B **50**, 1541 (1994).